

An Investigation of the Impact of Molecular Geometry upon Microcapsule Self-Assembly

Raymond J. Bergeron,^{*,§} Guo Wei Yao, Gregory W. Erdos,[†] Sam Milstein,[‡] Fenglan Gao,[§] William R. Weimar,[§] and Otto Phanstiel IV[§]

Contribution from the Department of Medicinal Chemistry, University of Florida, J. Hillis Miller Health Center, Gainesville, Florida 32610, Electron Microscopy Core Laboratory, Interdisciplinary Center for Biotechnology Research, University of Florida, Gainesville, Florida 32611, and Emisphere Technologies, Inc., 15 Skyline Drive, Hawthorne, New York 10532

Received November 7, 1994[⊗]

Abstract: Bis-amide dicarboxylic acids derived from the condensation of malonic acid, 1,1-dimethylmalonic acid, 1,1-cyclopropane dicarboxylic acid, or maleic acid with L-phenylalanine, (L-Phe), are shown to supramolecularly self-assemble in aqueous solution. When basic solutions of these diacids are taken to pH 2.4, microcapsules are formed. Scanning and transmission electron micrographs confirm that microcapsules and not solid microspheres are generated. The ability of these assemblies to encapsulate other materials present during their formation in water was demonstrated with a tannic acid marker. Structure–activity studies clearly demonstrate the importance of a *cis* geometry between L-Phe fragments for self-assembly. Molecular modeling revealed that the *cis* geometry of **1a**, **5a**, and **14** imparts a helical structure to these systems. The subsequent self-association via hydrogen bonds of these hydrophobic helical diacids is postulated as the mechanism for their self-assembly. Nonmicrocapsule forming scaffolds (predicated on oxalic, fumaric, and succinic acid backbones) favored “cuplike” or pocket geometries which were not conducive to intermolecular aggregation.

Introduction

Recent observations that organic molecules self-assemble into novel macromolecular constructs have generated new interest in the mechanism responsible for such associative processes.¹ Several unique supramolecular structures have been obtained using small organic building blocks. For example, Ghadiri demonstrated that cyclic peptides with an even number of alternating L- and D-amino acids were able to form organic nanotubes.² Other investigators have used amphiphiles and bolaamphiphiles to generate stabilized spherical micelles and tubular vesicles.^{3–5} While the formation of such aggregates is fascinating, because of the size of the constituent molecules and their degrees of conformational freedom, it is difficult to identify the structural parameters in these building blocks responsible for self-assembly.

Although many of the studies have focused on nano- and microtubule formation, investigations of alternate architectures are likely to be of equal importance in elucidating the associative

mechanisms responsible for the formation of these systems. The identification of smaller molecules with fewer degrees of conformational freedom, which participate in these phenomena, would certainly be of value in mechanistic studies. Recently L-Asp-diketopiperazines appended with amino acid subunits were found to self-assemble into microcapsules.⁶ This behavior was unique *only* to those diketopiperazines with phenylalanine (Phe) subunits, **1a–c**, shown in Figure 1. Basic solutions of these diketopiperazines (at pH 7.7) generated microcapsules when the pH of the solution was lowered to 2.4. The assembly phenomenon was found to be sensitive to both solution pH and substrate concentration. A “protonation-induced” phase-ordered transition as the initiator of self-assembly was suggested.^{2,6}

When trifunctional amino acids such as L-Asp cyclize (to form diketopiperazines), they generate a bis-carboxylic acid platform with a *cis* geometry imparted by the chiral Asp components.⁷ The L-Asp diketopiperazine dicarboxylic acid was condensed with 2 mol of phenylalanine to give the self-assembling substrates **1a–c**. Interestingly, the chirality of the Phe pendant did not seem to be critical for the assembly process of **1a** as the racemic mixture also formed microcapsules. Consequently, a study aimed at assessing the contribution of reduced degrees of freedom and *cis* geometry in the self-assembly of small phenylalaninediamide dicarboxylic acids seemed in order.

In this report two groups of bis-amide dicarboxylic acids are studied: one predicated on malonic acid and its analogues and a second based on succinic acid and its derivatives.

Results and Discussion

Malonic Acid Amides. The significance of the *cis* orientation of the pendant Phe groups in microcapsule formation was

[†] Electron Microscopy Core Laboratory.

[‡] Emisphere Technologies, Inc.

[§] University of Florida.

[⊗] Abstract published in *Advance ACS Abstracts*, May 15, 1995.

(1) (a) Whitesides, G. M.; Mathias, J. P.; Seto, C. T. *Science* **1991**, *254*, 1312–1319. (b) Mathias, J. P.; Seto, C. T.; Simanck, E. E.; Whitesides, G. M. *J. Am. Chem. Soc.* **1994**, *116*, 1725–1736. (c) Zerkowski, J. A.; MacDonald, J. C.; Seto, C. T.; Wierda, D. A.; Whitesides, G. M. *J. Am. Chem. Soc.* **1994**, *116*, 2382–2391.

(2) (a) Ghadiri, M. R.; Granja, J. R.; Milligan, R. A.; McRee, D. E.; Khazanovich, N. *Nature* **1993**, *366*, 324–327. (b) Ghadiri, M. R.; Granja, J. R.; Buehler, L. K. *Nature* **1994**, *369*, 301–304.

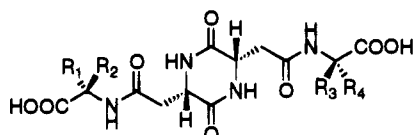
(3) (a) Fuhrhop, J. H.; Blumtritt, P.; Lehmann, C.; Luger, C. *J. Am. Chem. Soc.* **1991**, *113*, 7437–7439. (b) Svenson, S.; Kirste, B.; Fuhrhop, J. H. *J. Am. Chem. Soc.* **1994**, *116*, 11969–11975. (c) Andre, C.; Luger, P.; Bach, R.; Fuhrhop, J. H. *Carbohydr. Res.* **1995**, *266*, 15–35.

(4) (a) Frankel, D. A.; O'Brien, D. F. *J. Am. Chem. Soc.* **1991**, *113*, 7436–7437. (b) Frankel, D. A.; O'Brien, D. F. *J. Am. Chem. Soc.* **1994**, *116*, 10057–10069.

(5) Fuhrhop, J. H.; Spiroski, D.; Boettcher, C. *J. Am. Chem. Soc.* **1993**, *115*, 1600–1601.

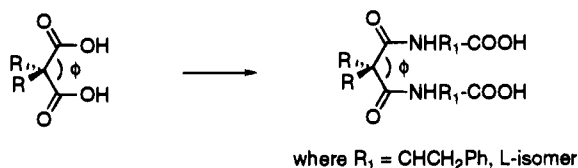
(6) Bergeron, R. J.; Phanstiel IV, O.; Yao, G. W.; Milstein, S.; Weimar, W. R. *J. Am. Chem. Soc.* **1994**, *116*, 8479–8484.

(7) Lannom, H. K.; Dill, K.; Danarie, M.; Lacombe, J. M.; Pavia, A. A. *Int. J. Peptide Protein Res.* **1986**, *28*, 67–78.

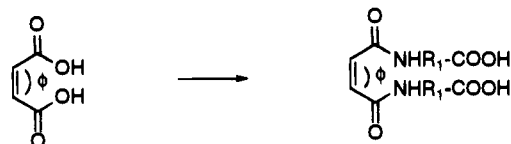


- 1a: $R_1, R_4 = \text{CH}_2\text{Ph}; R_2, R_3 = \text{H}$
 1b: $R_1, R_4 = \text{H}; R_2, R_3 = \text{CH}_2\text{Ph}$
 1c: $R_1, R_2, R_3, R_4 = \text{either } \text{CH}_2\text{Ph or H};$
 where $R_1 \neq R_2$ and $R_3 \neq R_4$

Figure 1. L-Asp diketopiperazine constructs which self-assemble into microcapsules.



- 5a: $R = \text{H}; \phi = 110^\circ$
 5b: $R = \text{CH}_3; \phi = 106^\circ$
 5c: $R = \text{cyclo } \text{CH}_2; \phi = 118^\circ$



14: $\phi = 60^\circ$



7: $\phi = 180^\circ$

Figure 2. Ligand orientation angle ϕ imparted by bis acid platforms.

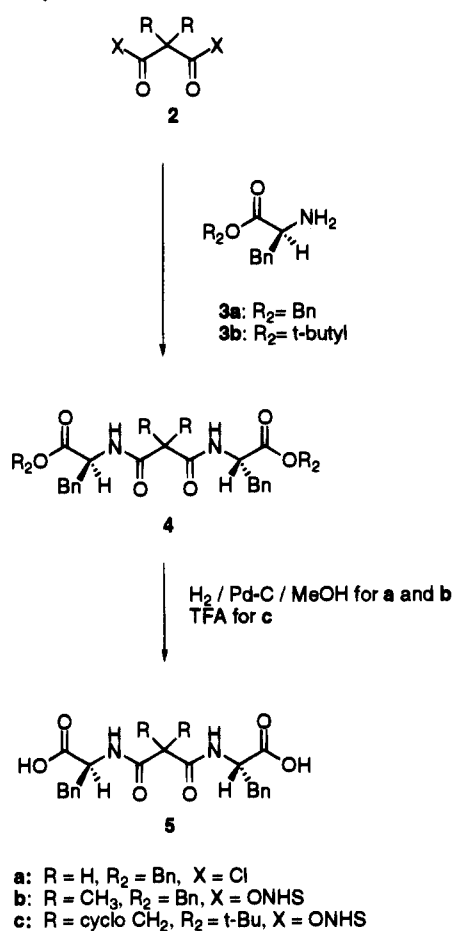
first evaluated by constructing Phe diamides of malonic acid, 1,1-dimethylmalonic acid, and 1,1-cyclopropane dicarboxylic acid. We elected to maintain phenylalanine (Phe) as the amino acid pendant in this investigation as earlier studies clearly pointed to its importance in microcapsule-forming diketopiperazines. Even though previous investigations indicated that racemic Phe could be used, L-Phe was chosen because of the commercial availability of its benzyl and *tert*-butyl esters and because only one diastereomeric bisamide product was expected.

These malonic derivatives (**5a–c**) represent Phe diamides, which are separated by a single carbon spacer and whose relative angular orientation is fixed in space. For example, the angular orientation of the L-Phe amide pendants of malonic derivative **5a** is fixed by the tetrahedral geometry of the central CH_2 spacer (Figure 2). In fact the *cisoid* relationship⁸ imparted by the malonic backbone place the Phe groups as close as is possible in a *cis* diamide framework. While all of the malonamides (**5a–c**) have a single carbon spacer and *cisoid* orientation⁸ of their Phe groups, the calculated angle between the amide carbonyls (defined here as ϕ) varies.

The replacement of the hydrogen atoms on the central methylene of **5a** with methyls (**5b**) or its incorporation into a

(8) We are using these terms (*cis* and "*cisoid*") not in the classical sense, but in an attempt to convey that the Phe pendants are oriented toward each other. We recognize that these terms are not normally applied to tetrahedral geometries.

Scheme 1. Synthesis of Malonic Acid Derivatives



cyclopropyl ring (**5c**) allowed for perturbation of the angle ϕ , while keeping the spacer unit constant. As shown in Figure 2, the angle ϕ is decreased by the steric demands of the geminal methyl groups in **5b** and increased by the rehybridization requirements of **5c**.⁹ Modeling studies utilizing a BIOSYM program¹⁰ identified the angles of **5a–c** as 110° , 106° , and 118° , respectively. Therefore, compounds **5a–c** allowed for the evaluation of microcapsule formation in systems, which had the L-Phe pendant groups all in close proximity to each other with ϕ angles varying by as much as 12° .

Attempts to access these rather simple substrates by direct condensation of the geminal acids (1,1-dimethylmalonic acid and 1,1-cyclopropane dicarboxylic acid) with L-Phe esters using the Yamada reagent, diphenylphosphoryl azide (DPPA),¹¹ were not highly successful with yields of $<10\%$ of the desired bis-amides **4b** and **4c** (Scheme 1). The efficiency of this coupling (where $R = \text{Me}$ or cyclo CH_2) was improved substantially (up to 77% yield) by generating the bis-activated *N*-hydroxy succinimide (NHS) ester of the acids, **2b** and **2c**, prior to reaction with the respective L-Phe esters **3a** and **3b**. Curiously, reaction of the NHS ester of the parent malonic acid and L-Phe benzyl ester gave only a 5% yield of the bis-amide **4a**. For this reason malonyl chloride was condensed with L-Phe benzyl ester to give **4a** in 23% yield. Subsequent deprotection of the terminal ester groups, either by hydrogenolysis of the benzyl ester¹² or by collapse of the *tert*-butyl ester with trifluoroacetic acid,¹³ gave

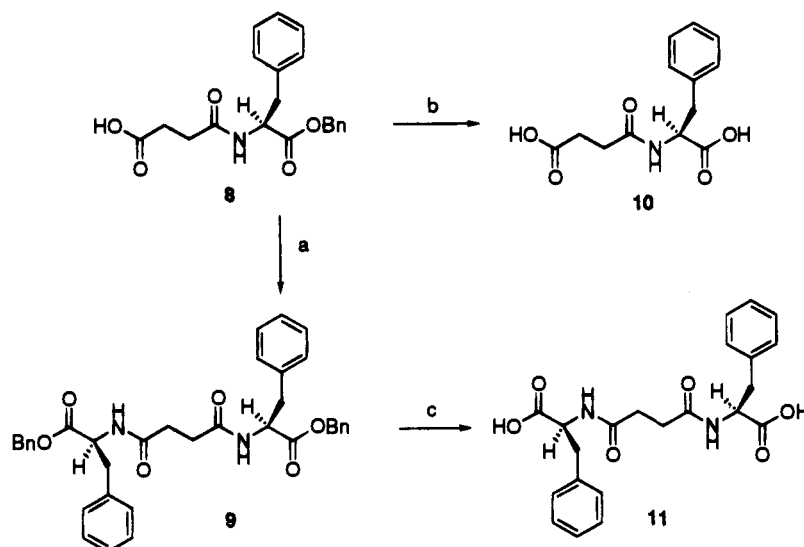
(9) Weigert, F. J.; Roberts, J. D. *J. Am. Chem. Soc.* **1967**, *89*, 5962.

(10) BIOSYM programs are available from Biosym Technologies, 9685 Scranton Road, San Diego, CA 92121-3752, (619)-458-9990.

(11) Shioiri, T.; Ninomiya, K.; Yamada, S. *J. Am. Chem. Soc.* **1972**, *94*, 6203–6205.

(12) Hartung, W. H.; Simonoff, R. *Org. React.* **1953**, *VII*, 263–326.

(13) Bryan, D. B.; Hall, R. F.; Holden, K. G.; Huffmann, W. F.; Gleason, J. G. *J. Am. Chem. Soc.* **1977**, *99*, 2353.

Scheme 2. Synthesis of 1,4-Butanedicarboxylic Acid Derivatives **10** and **11**^a

^a Reagents: a. BOP, L-Phe Bn ester, DIEA, room temperature; b and c. H₂, Pd-C, MeOH.

the free bis acids **5a–c** in 74%, 74%, and 67% yield, respectively.

Succinic Acid Amides. Construction of Phe diamides from succinic, maleic, and fumaric acid frameworks allowed for further assessment of the significance of both *cis* orientation and increased spacing of the Phe pendants in supramolecular self-assembly. In these systems the Phe groups were separated by a two carbon bridge. The insulating bridge was either rigid as with the *cis* and *trans* maleic and fumaric acid amides or mobile as with the succinic acid amide. In addition, a single Phe was affixed to a succinic acid framework in order to evaluate the microcapsule forming properties of a dicarboxylic acid containing only one Phe amide pendant.

The succinic acid derivatives were synthesized stepwise by reaction of L-Phe benzyl ester and succinic anhydride. The mono amide acid **8** was condensed with a second equivalent of L-Phe benzyl ester in the presence of BOP to give bis-amide **9** (Scheme 2). Subsequent removal of the benzyl esters of **8** and **9** by hydrogenation gave the mono (L-Phe) diacid **10** and the bis (L-Phe) diacid **11**, respectively. DPPA promoted condensation of L-Phe *tert*-butyl ester and maleic acid provided bis-amide **12** in 11% yield. The coupling yield was improved significantly with the BOP reagent.^{14,15} In this manner both the maleic diamide **12** (54%) and fumaric diamide **13** (84%) were accessed. Treatment of the *tert*-butyl esters (**12** and **13**) with TFA¹³ yielded the respective free acids **14** and **15** in 99% and 90% yield.

Oxalic Acid Amide. Finally, in hopes of further defining the distance requirements of the Phe subunits in systems which undergo microcapsule formation, the L-Phe diamide of oxalic acid was generated. Its self-assembly properties were then compared with those of the corresponding malonic and succinic acid homologues. The oxalic acid-bis(L-Phe) conjugate **7** was synthesized in 54% overall yield by direct condensation of oxalic acid and L-Phe benzyl ester with DPPA to give benzyl ester **6**, followed by deprotection of the benzyl ester with H₂ over 10% Pd-C.

Microcapsule Formation. Each of the diacid substrates **1a**, **5a–c**, **7**, **10**, **11**, **14**, and **15** was subjected to our microcapsule-forming protocol (see Experimental Section). However, as shown in Table 1, only compounds **1a**, **5a–c**, and **14** generated microcapsules under these conditions.

(14) Castro, B.; Dormoy, J. R.; Evin, G.; Selve, C. *Tetrahedron Lett.* **1975**, 1219.

(15) Castro, B.; Dormoy, J. R.; Dourtoglou, B.; Evin, G.; Selve, C.; Zeigler, J. C. *Synthesis* **1976**, 715.

Table 1. Microcapsule Formation Results

compd no.	estimated ligand orientation angle (ϕ)	bis acid backbone	microcapsule test observations
1a	97°	L-Asp diketopiperazine	microcapsules
5a	110°	malonic acid	microcapsules
5b	106°	1,1-dimethyl malonic acid	microcapsules
5c	118°	1,1-cyclopropane dicarboxylic acid	microcapsules
7	180°	oxalic acid	crystalline ppt.
10		1,4-butane dicarboxylic acid	amorphous ppt.
11		1,4-butane dicarboxylic acid	amorphous ppt.
14	60°	maleic acid	microcapsules
15	180°	fumaric acid	amorphous ppt.

Table 2. Concentration, pH, and pK_a Parameters for Microcapsule-Forming Compounds

compd no.	concn ^a (mM)	pH ^b	pK _{a1}	pK _{a2}
1a	40	3.30	4.00	4.90
5a	30	3.26	3.67	4.70
5b	25	3.26	3.55	4.62
5c	13	3.26	3.53	4.50
14	23	3.26	3.70	4.87

^a Concentration of amide above which a dense suspension (%T < 0.5) of microcapsules is formed in the presence of 500 mM citric acid (pH 2.4). ^b pH above which %T is >95% at an amide concentration of 50 mM in 500 mM Li citrate.

Our previous investigations with the diketopiperazine systems **1a–c** revealed a sharp dependence of the assembly process on substrate concentration and solution pH.⁶ For comparison purposes we determined the impact of these parameters on the self-assembly of compounds **5a–c** and **14**. Each compound was evaluated by monitoring the change in solution turbidity, while altering the pH at a fixed Phe amide concentration or by holding the pH constant and varying the concentration of the amide substrate (Table 2). Each concentration dependence was determined in 500 mM citric acid from a plot of the solution transmittance (%T) vs concentration. For example as illustrated in Figure 3, compound **5a** demonstrated a sharp transition from a clear solution (>95% T) to a dense suspension of microcapsules (0.2%T) at concentrations of **5a** above 30 mM. The influence of pH on solution turbidity was studied in solutions containing 50 mM **5a** in 500 mM lithium citrate buffers (Figure 4). The percent transmittance (%T) was <0.5% at pH 2.67 and >95% at pH 3.26. The pK_as of **1a**, **5a–c**, and **14** were

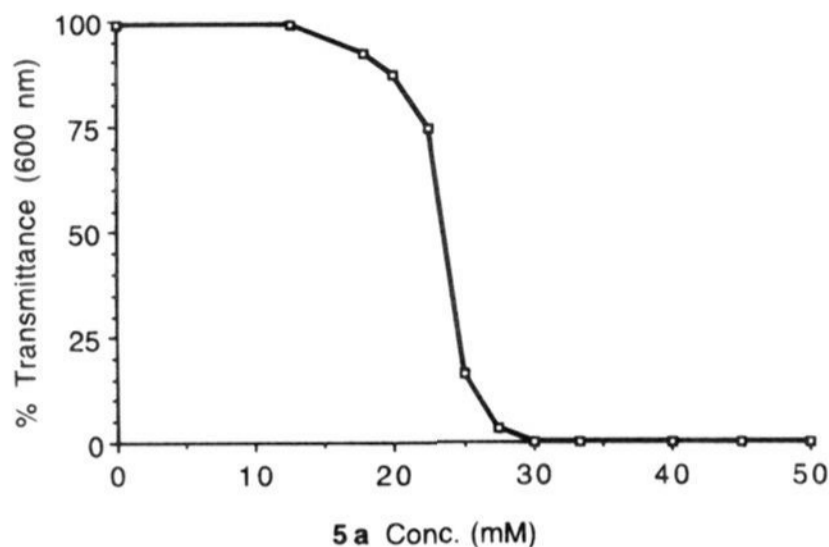


Figure 3. Percent of transmittance (at 600 nm) vs concentration of **5a** in 500 mM citric acid.

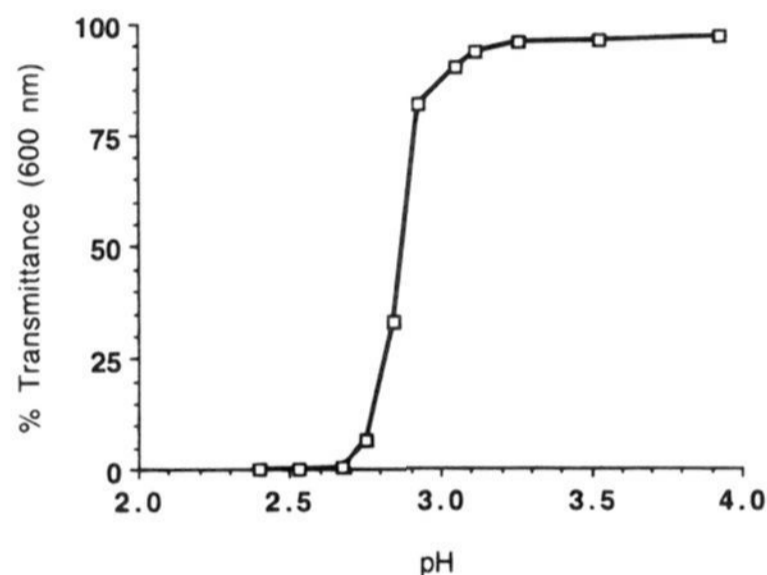


Figure 4. Percent of transmittance (at 600 nm) vs pH measurements with 50 mM **5a** and 500 mM lithium citrate.

determined by titration of each Phe amide substrate, and the values are listed in Table 2. As expected, the pK_a s of these Phe diamide diacids were all very similar.

The experimental data are consistent with the "protonation induced" assembly process postulated in our earlier paper.⁶ The visible manifestation of the supramolecular capsules (i.e., turbidity) is only apparent when the starting dianion is acidified to the fully protonated species in greater than ca. 95%. It is possible that the carboxylate anions actually hinder self-assembly by the electrostatic repulsion of like charges. From our pK_a and pH measurements we estimate that one anionic species per 30 molecules of **5a** is sufficient to abort supramolecular assembly.

However, if protonation was the only important parameter, substrates with similar pK_a s would demonstrate the same pH and concentration dependence. This is certainly true for the pH dependence of the microcapsule-forming substrates in this study (**1a**, **5a–c**, **14**) as each generates microcapsules at a pH well below their measured pK_a s. However, the compounds show different concentration dependences (**5c**: 13 mM vs **5a**: 30 mM). This difference may be due to the solubility of the microcapsules generated by each substrate or of the acid substrate itself. These results are in agreement with the findings of Ghadiri, wherein the insolubilities of the regenerated acids were shown to play an important role in the assembly process.²

As shown in Table 1, all of the malonic derivatives (**5a–c**) formed microcapsules as determined by light microscopy. Since the microcapsules generated by **5c** under our standardized conditions gave a high density of microcapsules from low concentrations of **5c** substrate (Table 2, **5c**: 13 mM), they were selected for study at higher magnification. Scanning electron micrographs (SEMs) were obtained for compound **5c** (Figure

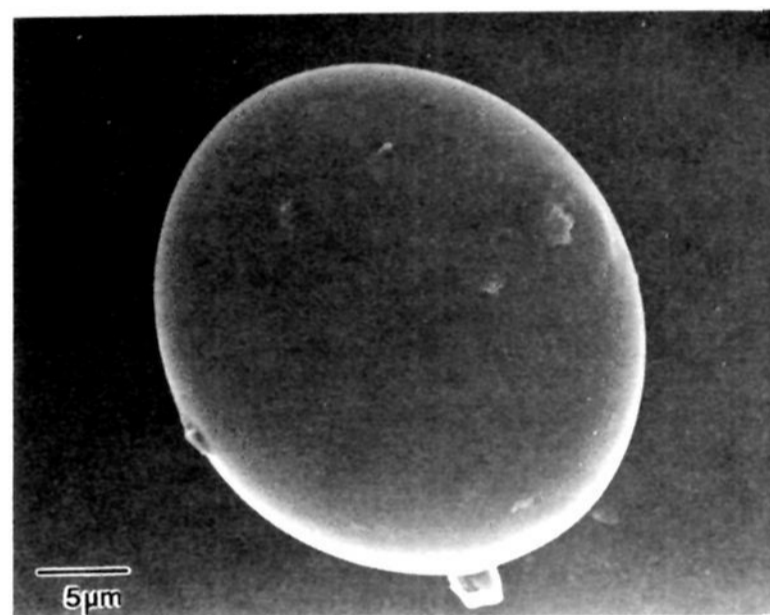
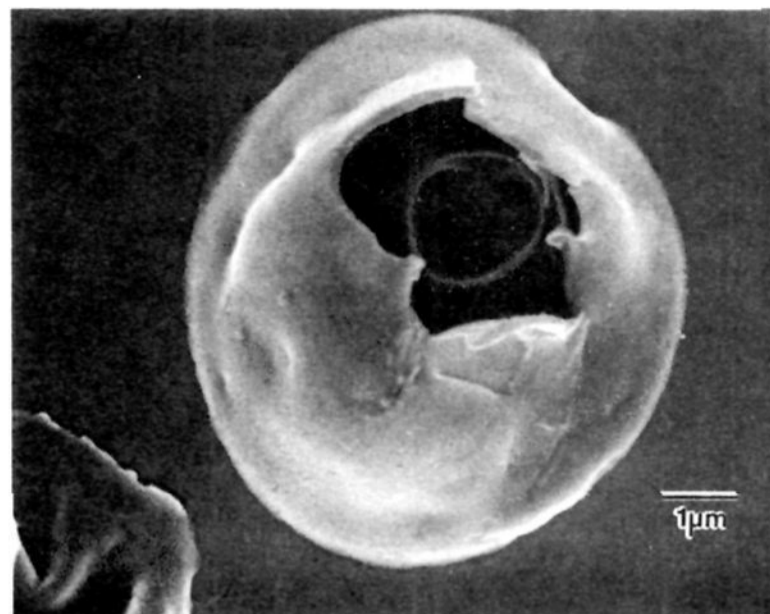


Figure 5. SEM micrographs of microcapsules generated from compound **5c**.

5) and confirmed that microcapsules and not solid microspheres were generated. Estimates of the microcapsule shell thickness (150 nm) would require approximately 100 molecules of **5c** oriented end-to-end to traverse the microcapsule shell. However, a stacking of the bis amides seems more likely. A stacked array would allow for a greater number of stabilizing intermolecular hydrogen bonds and would require a greater number of assembled tetrapeptides to traverse the capsule shell.

The ability of these microcapsules, while undergoing self-assembly, to entrap other substrates present in the solution was verified with transmission electron microscopy (TEM). To visualize the entrapment phenomenon directly, tannic acid was chosen for its diagnostic staining properties. Microcapsules were generated from a solution containing compound **5c** and tannic acid by lowering the pH from 7.7 to 2.4 with a citric acid solution. TEM micrographs clearly show that the tannic acid was entrapped inside the microcapsule (Figure 6). It is notable that the self-recognition of **5c** fragments must be energetically favorable enough during the assembly process, that the presence of tannic acid does not interfere with the formation of microcapsules.

The molecular fidelity observed during the aggregation process is in good agreement with the reversible assembly processes postulated by Whitesides.¹ He theorized that one method of self-assembly involves association by many weak, reversible interactions that result in a final structure which is a thermodynamic minimum. Furthermore, unrecognized substrates (such as tannic acid) should be rejected during this dynamic equilibria process. Our TEM findings are consistent with this premise as little tannic acid is incorporated into the microcapsule shell depicted in Figure 4. However, based on

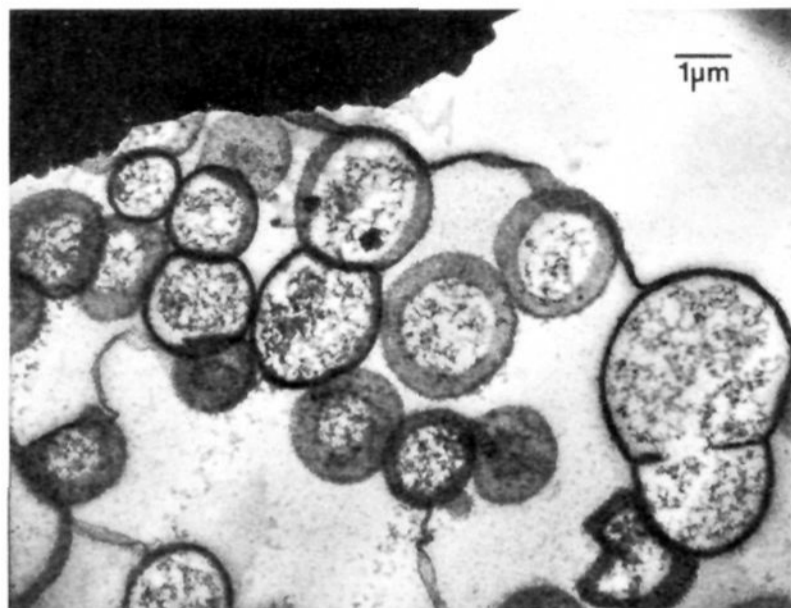


Figure 6. TEM micrograph of microcapsules generated from compound **5c** in the presence of tannic acid.

the electron microscopy alone, we cannot rule out the possibility that some tannic acid may be intercalated in the microcapsule wall. It should be noted that control runs without tannic acid were not able to be imaged by this technique because of the apparent mechanical instability of the empty microcapsules during preparation. Nevertheless, the presence of tannic acid does not disrupt the formation of microcapsules.

Of the succinic acid Phe-diamides only the maleic acid based amide **14** formed microcapsules, while the succinic acid diamide **11** and the fumaric acid compound **15** generated an amorphous precipitate and crystalline solid, respectively. Compound **10**, the monoamide analogue of **11**, also formed an amorphous precipitate.

The influence of the bond distance separating the Phe amides upon microcapsular self-assembly seems apparent when comparing the diamide dicarboxylic acid series L-PheCO-(CH₂)_n-Co-L-Phe (with *n* = 0, 1, and 2). As described above, only compound **5a** (where *n* = 1) generated microcapsules. Interestingly, neither the oxalic derivative **7** nor succinic analogue **11** generated microcapsules. These results further support the importance of the *cis* relationship between the two Phe groups for self-assembly.

Spatial Orientation. Inspection of Table 1 reveals that those compounds which undergo self-assembly into microcapsules all have a critical angle (ϕ) in their diacid platform, which orients the Phe fragments toward each other. Moreover, this angle is fixed in all cases studied so far. For example, the *cis* diketopiperazine platform of compounds **1a–c** orient the Phe subunits ($\phi = 97^\circ$) in a fixed geometry. Likewise, compounds **5a–c** (with $\phi_c = 118^\circ$, $\phi_a = 110^\circ$, $\phi_b = 106^\circ$, respectively) orient the Phe pendants toward each other with a locked geometry imparted by the tetrahedral carbon spacer.

The lack of a fixed spatial orientation of the Phe pendants in compound **11** can be used to rationalize why this compound does not self-assemble, even though it possesses sufficient tether length and conformational flexibility. This requirement of having a rigid *cis* orientation is further illustrated with the maleic and fumaric acid platforms. As shown in Table 1, the maleic acid-bis Phe conjugate **14** ($\phi = 60^\circ$) generated microcapsules, whereas the isomeric fumaric derivative **15** ($\phi = 180^\circ$) did not. These platforms are unique in that they approximate the eclipsed Phe and anti Phe rotamers of compound **11**. The fact that only the maleic construct **14** ($\phi = 60^\circ$) forms microcapsules further underscores the importance of attaining a fixed *cis* geometry.

Molecular Modeling. In an attempt to generate a model which might help explain why these compounds aggregate into supramolecular arrays, we minimized the conformations of each peptide using the INSIGHT and DISCOVER programs provided

by BIOSYM.¹⁰ The lowest energy minima was selected by comparing the energy of each conformation obtained from a dynamic simulation of each structure at 300 K.

Remarkably, the microcapsule-forming peptides (**1a**, **5a–c**, **14**) all formed helical structures with their carboxyl groups oriented away from the hydrophobic central core. The helical conformations found for **1a**, **5a**, and **14** are depicted in Figure 7. Our preliminary dynamic studies of these conformations showed other conformations which were close in energy to those depicted. These alternate structures are also helical and have one seven-membered H-bond between one of the terminal carboxyls and the carbonyl of the Phe amide. Since nearly identical helical conformations were found with and without this seven-membered hydrogen bond, we believe it to be of secondary importance in the generation of the helix.

The modeling studies are in keeping with our earlier premise that the ligand orientation angle (ϕ) effects the assembly process. By locking in a *cis* geometry⁸ the scaffolds of **1a**, **5a**, and **14** allow the peptide to complete the helical turn necessary for generation of the hydrophobic helix. We speculate that acidification of the terminal carboxylates allows for intermolecular hydrogen bonding (between different helical subunits) thereby generating the observed larger arrays (see Figure 8). This insight is consistent with our earlier observations that anionic species (R-COO⁻, a non H bond donor) can disrupt the putative assembly process.

The nonmicrocapsule forming materials (**7**, **10**, **11**, and **15**) gave linear and pocket-like structures. Our minimized structures (for **7**, **11**, and **15**) are illustrated in Figure 9. The linear geometry of peptide **7** is imparted by the rigid oxalic spacer ($\phi = 180^\circ$) which orients the hydrophobic Phe ligands in opposite directions. Likewise, the fumaric derivative **15** ($\phi = 180^\circ$) separates the hydrophobic Phe ligands by a longer carbon spacer. This increased distance allows the amide groups to twist slightly out of the conjugation plane to accommodate a seven-membered H bond with the terminal COOH. Due to the flexible CH₂CH₂ spacer of the succinic derivative **11**, one may have expected **11** to adopt a conformation which was similar to fumarate **15** or its maleic counterpart **14**. However, each of these conformations would require **11** to adopt a higher energy eclipsed conformer. The succinic moiety **11** adopted a pocket structure with the phenyl rings pointed away from each other. The flexible ethyl spacer of **11** prefers a staggered conformation and contributes to the formation of a pocket geometry. It is of course possible that these conformations may be significantly altered during the assembly of two or more species in an aqueous environment. Nevertheless, the proposed model fits all of our experimental data on these microcapsule-forming systems.

Conclusions

Based on this study there seems to be several structural criteria that these low molecular weight diamides should possess in order to undergo microcapsule self-assembly. First, there should be a certain tether length between the Phe pendants in order to attain the required geometry for molecular packing. Second, the bis acid platform must orient the Phe subunits with a certain angle ϕ (e.g., between 60° and 120°). Third, and perhaps most vital, is that this angle be fixed in space. To date we have observed that only those substrates which have a *cis* geometry undergo this type of self-assembly. This spatial orientation can be attained either through reduced conformational flexibility (with rings or *cis* double bonds) or by using other fixed geometries imparted by the diacid platform itself (e.g., the tetrahedral geometry imparted by the central sp³ hybridized carbon of **5a**). The significance of the reduced degrees of freedom (rigidity) in these amides, while in keeping with a major

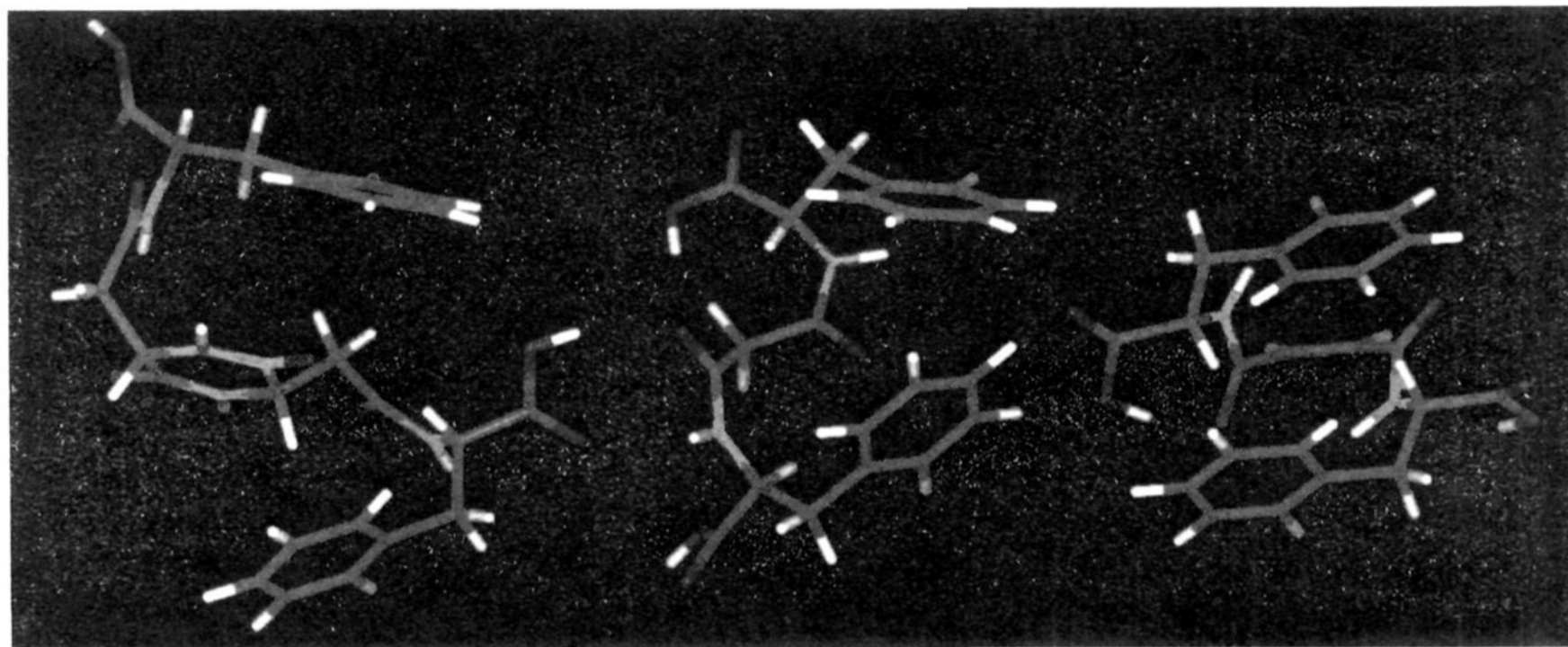


Figure 7. BIOSYM generated structures of peptides 1a, 5a, 14.

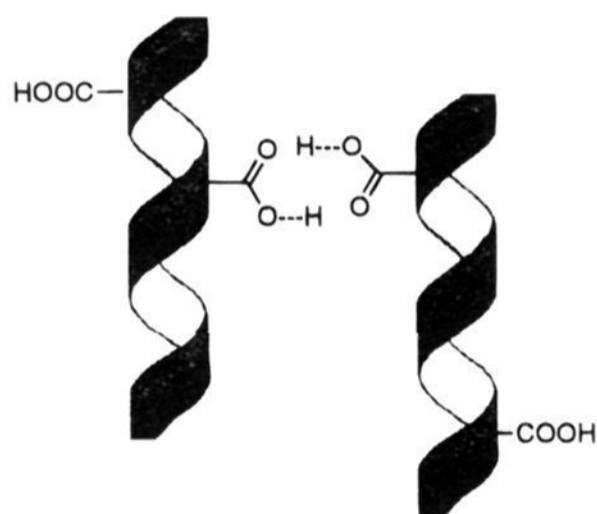


Figure 8. Proposed association of helical diacids.

entropy contribution to microcapsule formation, must be further evaluated. Our current findings with diamide diacids of Phe are consistent with the idea that molecules that undergo assembly into microcapsular geometries must possess critical tether distances with a fixed angular orientation ($\phi = 60$ to 120°) of Phe subunits. These structural requirements are necessary for the generation of helical conformations with the carboxylic acid pointed away from the central hydrophobic core. How these helical diacid motifs interact and self-associate will be explored in future studies using NMR and CD measurements.

Experimental Section

General Method. All reagents were purchased either from the Aldrich Chemical Co. or the Sigma Chemical Co. and were used without further purification. Silica gel 40 mm, obtained from J. T. Baker, was used for flash column chromatography. ^1H NMR spectra were recorded at 300 MHz and ^{13}C NMR were recorded at 75 MHz. Chemical shifts are given in parts per million downfield from an internal tetramethylsilane standard. Mass spectra were carried out on a Kratos MS 80RFA or a Finnigan 4516 MS instrument. Optical rotations were run at 589 nm (the Na D-line) on a Perkin-Elmer 241 polarimeter, with c expressed as g of compound per 100 mL. Elemental analyses were performed by Atlantic Microlabs, Norcross, GA. Melting points were uncorrected. Light microscopy was performed on a camera mounted-ZEISS light microscope. SEM pictures were obtained on a Hitachi 4000 scanning electron microscope and TEMs were done on a Hitachi 7000 transmission electron microscope.

Modeling Parameters. The modeling studies were conducted with BIOSYM software¹⁰ running on a Silicon Graphics Indigo² workstation. The molecules were built using standard amino acid templates, bond lengths, angles, and side chain dihedral angles. The atoms within each molecule were assigned their proper hybridization, charge, and bond order utilizing the Builder module of Insight (Version 2.3.1). The

CVFF forcefield provided by the Discover module was chosen for the minimization constraints. This forcefield was applied to the constructed peptide and evaluated with two methods (i.e., the steepest descent and conjugate gradient methods). The interaction number for the steepest descent method was 100 and 200 for the conjugate gradients method. The derivative (or convergence criterion) was chosen as 0.001 Kcal/mol-Å. The conformational preference of each peptide was determined in the following manner: the peptide underwent 1000 steps of a dynamic simulation at 300 K with a time interval of 1.0 fs. The resulting lowest energy conformation was selected as the minima for this parameter set and is depicted in either Figure 7 or 9.

Preparation of Microcapsules. The bis acid (0.01 mmol) is dissolved in 0.1 mL of aqueous Li_2CO_3 (0.1 M) to give a clear solution of the lithium salt in deionized water with a pH typically between 6.8 and 8.0. Fifty microliters of this 0.1 M solution is mixed with 50 μL of 1 M aqueous citric acid and shaken. A white suspension was generated. Microscopic examination of the suspension revealed the formation of tiny spheres. A wide size distribution was observed qualitatively (ranging from 10 μm to submicron diameters).

Concentration and pH Dependence Studies. A stock solution containing the lithium salt of the diamide was prepared by stepwise addition of exactly 2 equiv of a standardized solution of LiOH (stored under argon to prevent precipitation of lithium carbonate). The final concentration of the dilithium salt of the diamide was 100 mM, and the pH was always between 7.0 and 8.0. The solution was filtered through a 0.2 μm membrane prior to use. For concentration dependence studies, an appropriate amount of the 100 mM stock solution was diluted with deionized water to 500 μL . Microcapsule formation was then initiated by addition of an equal volume of 1 M citric acid, so that the final concentration ranged from 0 to 50 mM dilithium diamide in 500 mM citric acid with the pH below 2.5. Turbidity was assessed over this range of concentrations by measuring percent transmittance at 600 nm (Figure 3). For pH dependence studies, 500 μL of 100 mM dilithium diamide solution was mixed with an equal volume of one of a series of 1 M lithium citrate buffers containing between 0 and 1 equivalent of lithium hydroxide so that the final measured pH of the mixture ranged from ca. 2.4–4.0. Turbidity was assessed over this pH range by measuring percent transmittance at 600 nm (Figure 4).

Scanning Electron Microscopy (SEM). We elected to use the sodium salt of the peptide 5c for our electron microscopy studies as it generated larger spheres than the corresponding lithium salt according to our light microscopy observations. A typical procedure involved the generation of a white suspension by combining 100 μL of 0.43 M citric acid and 50 μL of a 0.1 M aqueous solution of the sodium salt of the peptide. The aqueous suspension was deposited on polylysine-coated glass coverslips and fixed with 2% OsO_4 for 4 h. The sample was washed with distilled water, air dried, and sputter coated with gold. SEM photographs were then obtained.

Tannic Acid Entrapment Experiment Using Transmission Electron Microscopy (TEM). A typical procedure involved the generation of a white suspension by adding a solution containing 50 μL of 0.86 M citric acid and 50 μL of 3 wt% tannic acid to 50 μL of a 100 mM

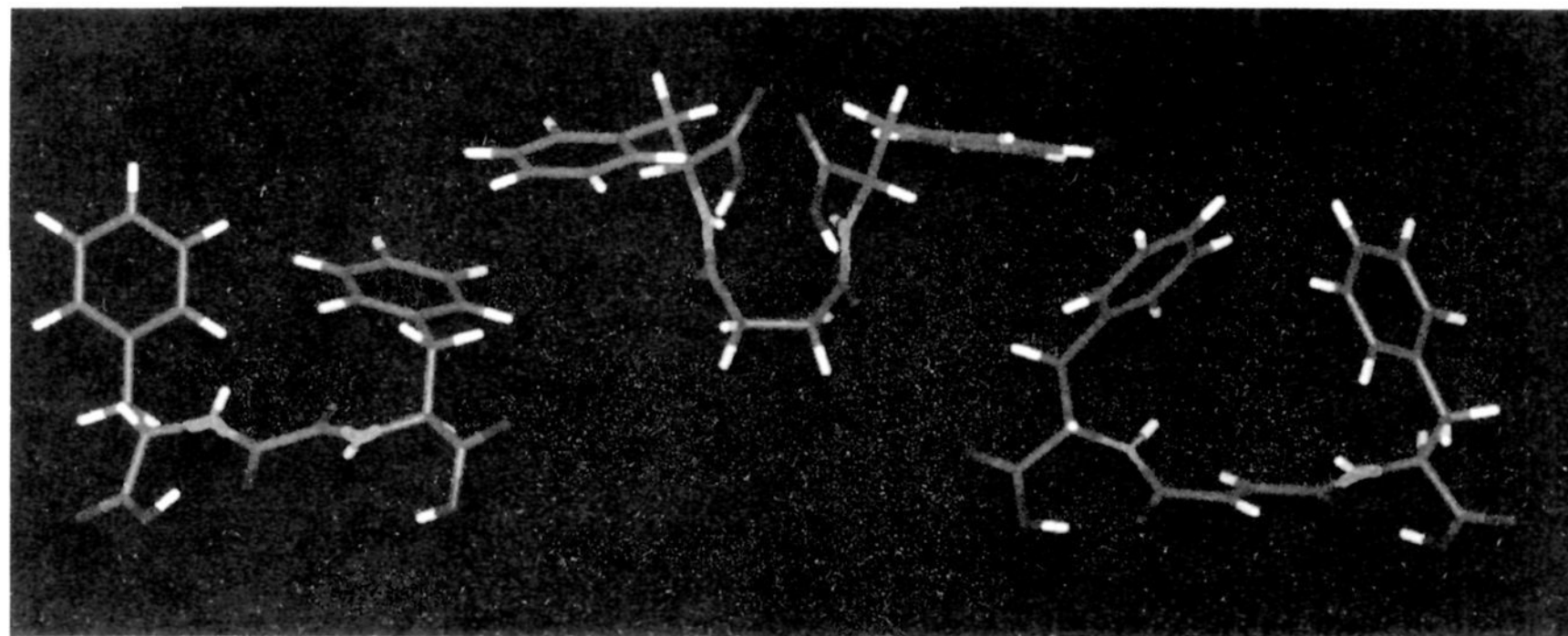


Figure 9. BIOSYM generated structures of peptides 7, 11, and 15.

aqueous solution of the sodium salt of the peptide. The aqueous solution was deposited on a Nucleopore filter and fixed with 4% OsO₄ for 4 h. The sample was washed with distilled water, and 95% EtOH and air dried. The sample was dispersed in 100% LR white resin and polymerized in an oven at 60 °C. TEM photographs were then obtained.

Bis(N α -amido-L-phenylalanine benzyl ester) malonate (4a). L-phenylalanine benzyl ester (*p*-toluenesulfonate salt) (12.5 g, 29.2 mmol) was suspended in 100 mL of CH₂Cl₂, and triethylamine (TEA, 7.4 g, 73.1 mmol) added. The yellow solution was cooled to 0 °C, and malonyl chloride (2.0 g, 14.2 mmol) was added dropwise under a N₂ atmosphere. After the addition was complete the solution was warmed to room temperature and stirred overnight. The orange solution was washed successively with aqueous NaHCO₃, water, 1 N HCl and water until pH = 6. The organic layer was separated, dried over anhydrous MgSO₄, filtered, and concentrated to give an orange oil (6.2 g). Column chromatography (40% ethyl acetate/hexane) gave the pure dibenzyl ester **4a** (1.92 g, 23%): mp = 93–94 °C; ¹H NMR (CDCl₃) δ 7.30 (m, 22H), 5.10 (q, 4H, CH₂), 4.88 (dd, 2H, CH), 3.13 (m, 6H, CH₂); optical rotation [α]_D²² 19° (*c* 0.5, CHCl₃). Anal. Calcd for C₃₅H₃₄N₂O₆: C, 72.65; H, 5.92; N, 4.84. Found: C, 72.49; H, 5.91; N, 4.79.

Bis(N α -amido-L-phenylalanine benzyl ester) 1,1-dimethyl malonate (4b). Dimethyl malonic acid (5.15 g, 39 mmol) and *N*-hydroxy succinimide (NHS, 9.58 g, 83 mmol) were dissolved in anhydrous THF (150 mL). The cloudy suspension was cooled to 0 °C, and a solution of dicyclohexylcarbodiimide (DCC, 4.04 g, 19.6 mmol) in 75 mL of dry THF was added dropwise over 30 min. The ice bath was removed, and the solution was allowed to warm to room temperature and stirred overnight. The solution was filtered and concentrated. The crude *N*-hydroxy succinimide (NHS) ester was suspended in dry THF and cooled to 0 °C. L-Phenylalanine benzyl ester *p*-toluenesulfonate salt (34.2 g, 80 mmol) was dissolved in CHCl₃ and washed with aqueous NaHCO₃. The organic layer was separated, dried over anhydrous MgSO₄, filtered, and concentrated to give the free amine as an oil (19.0 g). The amine was dissolved in 50 mL of dry THF and added dropwise to the cooled suspension. The reaction was warmed to room temperature and stirred overnight. The volatiles were removed under reduced pressure and the residue was dissolved in CDCl₃, washed successively with 1 N HCl, water, aqueous NaHCO₃, and water. The organic layer was separated, dried over anhydrous MgSO₄, filtered, and concentrated to give a yellow oil (20.5 g). Column chromatography (30% ethyl acetate/hexane, SiO₂, *R*_f 0.37) gave pure **4b** (8.55 g, 36% overall): ¹H NMR (CDCl₃) δ 7.30 (m, 16H), 7.02 (m, 6H), 5.15 (q, 4H, CH₂), 4.80 (dd, 2H, CH), 3.09 (m, 4H, CH₂), 1.32 (s, 6H, CH₃); optical rotation [α]_D²² -8° (*c* 0.5, CHCl₃). Anal. Calcd for C₃₇H₃₈N₂O₆: C, 73.25; H, 6.31; N, 4.62. Found: C, 73.21; H, 6.37; N, 4.57.

Bis(N α -amido-L-phenylalanine *tert*-butyl ester) 1,1-cyclopropane dicarboxylate (4c). The bis *tert*-butyl ester **4c** was synthesized using the same procedure as **4b** except L-phenylalanine *tert*-butyl ester hydrochloride was used. 1,1-Cyclopropane dicarboxylic acid (3.24 g, 24.9 mmol) was reacted with DCC (11.3 g, 54.8 mmol) and NHS (6.31

g, 54.8 mmol) to give the crude bis NHS ester. The crude solid (9.0 g) was suspended in THF and cooled to 0 °C. L-Phenylalanine *tert*-butyl ester hydrochloride (14.07 g, 54.8 mmol) was converted to its free amine by the same procedure as described for **4b**. The amine (13.36 g) was dissolved in dry THF and added dropwise to the cooled suspension of the NHS ester. After stirring overnight and workup, column chromatography (35% ethyl acetate/hexane, *R*_f 0.34) gave the pure di-*tert*-butyl ester **4c** (10.35 g, 77%); ¹H NMR (CDCl₃) δ 7.50 (d, 2H, NH) 7.20 (s, 10H, aromatic), 4.67 (dd, 2H, CH), 3.06 (d, 4H, CH₂), 1.40 (s, 18H, *tert*-butyl), 1.23 (q, 4H, cyclopropyl); optical rotation [α]_D²² 48° (*c* 1.7, CHCl₃). Anal. Calcd for C₃₁H₄₀N₂O₆: C, 69.38; H, 7.51; N, 5.22. Found: C, 69.49; H, 7.47; N, 5.15.

Bis(N α -amido-L-phenylalanine) Malonate (5a). The dibenzyl ester **4a** (1.2 g, 2.07 mmol) was dissolved in MeOH (100 mL), and 10% Pd-C (0.35 g) added. The black suspension was degassed three times and hydrogen gas introduced. After 2 h the catalyst was filtered off and washed with MeOH. The filtrate was concentrated to give an oil (0.99 g). The crude product was purified by column chromatography (Sephadex LH-20, 15% EtOH/toluene) to give **5a** as a white solid (0.61 g, 74%): mp = 162–164 °C; ¹H NMR (CD₃OD) δ 7.22 (m, 10H, aromatic), 4.66 (dd, 2H, CH, *J* = 8 Hz, 5.3 Hz), 3.17 (s, 2H, CH₂), 3.16 (dd, 2H, diastereotopic CH₂, *J* = 13.8 Hz, 5.3 Hz), 2.99 (dd, 2H, diastereotopic CH₂, *J* = 13.8 Hz, 8.1 Hz); optical rotation [α]_D²² 52° (*c* 0.3, MeOH). Anal. Calcd for C₂₁H₂₂N₂O₆: C, 63.31; H, 5.57; N, 7.03. Found: C, 63.25; H, 5.59; N, 6.98.

Bis(N α -amido-L-phenylalanine) 1,1-Dimethyl Malonate (5b). Compound **5b** was prepared by hydrogenation of its dibenzyl ester **4b** (1.75 g, 2.88 mmol) using the same procedure as described for **5a** except the reaction was stirred for 3 h prior to workup. The crude solid (1.11 g) was purified by column chromatography (Sephadex LH-20, 15% EtOH/toluene) to give pure **5b** as a white solid (0.91 g, 74%): mp = 62–64 °C; ¹H NMR (CD₃OD) δ 7.20 (m, 10H, aromatic), 4.63 (m, 2H, CH), 3.25 (dd, 2H, CH₂), 3.01 (dd, 2H, CH₂), 1.18 (s, 6H, CH₃); optical rotation [α]_D²² -2° (*c* 1, MeOH). Anal. Calcd for C₂₃H₂₆N₂O₆: C, 64.78; H, 6.14; N, 6.57. Found: C, 64.67; H, 6.20; N, 6.46.

Bis(N α -amido-L-phenylalanine) 1,1-Cyclopropane Dicarboxylate (5c). The bis *tert*-butyl ester **4c** (8.31 g, 15.5 mmol) was dissolved in CH₂Cl₂ (50 mL) and cooled to 0 °C. Trifluoroacetic acid (TFA, 20 mL) was added dropwise under a nitrogen atmosphere. After 80 min the volatiles were removed under reduced pressure to give a white solid. Column chromatography (Sephadex LH-20, 10% EtOH/toluene) gave the pure bis acid **5c** (4.4 g, 67%): ¹H NMR (*d*₆-DMSO) δ 12.83 (br s, 2H, COOH), 8.49 (d, 2H, NH), 7.20 (m, 10H, aromatic), 4.42 (m, 2H, CH), 2.97 (m, 4H, CH₂), 1.18 (s, 4H, cyclopropyl); high resolution mass spectrum theory 424.1634, found 424.1617; optical rotation [α]_D²¹ -3° (*c* 1, MeOH). Anal. Calcd for C₂₃H₂₄N₂O₆: C, 65.08; H, 5.70; N, 6.60. Found: C, 65.15; H, 5.79; N, 6.53.

Bis(N α -amido-L-phenylalanine benzyl ester) Oxalate (6). To a stirred solution of oxalic acid (0.23 g, 2.5 mmol) and L-phenylalanine benzyl ester *p*-toluenesulfonate salt (2.14 g, 5 mmol) in 15 mL of DMF

was added diphenyl phosphoryl azide (DPPA, 1.45 g, 5.25 mmol) dropwise at 0 °C. After 15 min triethylamine (TEA, 1.1 g, 10 mmol) was added dropwise, and the solution was allowed to warm to room temperature and stirred overnight. Removal of the volatiles under reduced pressure afforded an oil which was dissolved in CH₂Cl₂ and washed successively with 1 N HCl, water, aqueous NaHCO₃, and water. The organic layer was separated and dried over anhydrous MgSO₄, filtered, and concentrated to give a pale yellow oil. The oil was recrystallized from 30% EtOAc/hexane to give ester **6** as a white solid (0.76 g, 54%): mp = 158–159 °C; ¹H NMR (CDCl₃) δ 7.20 (m, 20H), 5.42 (m, 2H), 5.10 (d, 2H), 4.93 (m, 4H), 2.96 (d, 4H); ¹³C NMR (CDCl₃) 172.4, 156.0, 135.8, 135.1, 129.4, 128.6, 128.5, 128.4, 128.3, 126.8, 67.1, 53.9, 38.5; optical rotation [α]_D²⁵ 13° (c 1, CHCl₃). Anal. Calcd for C₃₄H₃₂N₂O₆: C, 72.33; H, 5.71; N, 4.96. Found: C, 72.56; H, 5.96; N, 5.10.

Bis(Nα-amido-L-phenylalanine) Oxalate (7). Compound **7** was prepared by hydrogenation of its dibenzyl ester **6** (0.56 g, 1 mmol) over 10% Pd–C (60 mg) in MeOH using the same procedure as described for **5a** except the reaction was stirred for 45 min prior to workup. Filtration of the catalyst and concentration of the filtrate gave acid **7** as a white solid (0.38 g, 100%): mp = 88–90 °C; ¹H NMR (CD₃OD) δ 7.25 (m, 10H), 4.51 (m, 2H), 3.05 (m, 4H); ¹³C NMR (d₆-DMSO) 173.6, 156.8, 137.3, 129.3, 128.1, 126.3, 53.9, 37.4; optical rotation [α]_D²⁵ 46° (c 1, MeOH). Anal. Calcd for C₂₀H₂₀N₂O₆: C, 62.49; H, 5.24; N, 7.29. Found: C, 62.14; H, 5.46; N, 7.60.

(Nα-amido-L-phenylalanine benzyl ester) Monosuccinate (8). To a stirred solution of L-Phe benzyl ester, *p*-toluenesulfonate salt (2.14 g, 5 mmol) in 20 mL of DMF and 20 mL of THF was added 4-methylmorpholine (1.12 mL, 12 mmol) dropwise at 0 °C. The resulting mixture was stirred for 30 min, and succinic anhydride (0.5 g, 5 mmol) in 5 mL of DMF was added. The reaction mixture was warmed to room temperature and stirred overnight. The solvents were removed *in vacuo*, and the resultant oil was dissolved in EtOAc and washed with water. The organic layer was separated, dried over anhydrous MgSO₄, filtered, and concentrated to give a white solid. Column chromatography (LH-20 Sephadex, 15% EtOH/toluene) provided the pure mono amide **8** (1.2 g, 78%): mp 108–109 °C; ¹H NMR (CDCl₃) δ 9.00 (br s, 1H), 7.05 (m, 10H), 6.30 (m, 1H), 5.10 (m, 2H), 4.91 (m, 1H), 3.07 (m, 2H), 2.63 (m, 2H), 2.45 (m, 2H); ¹³C NMR (CDCl₃) 177.0, 171.3, 171.2, 135.4, 134.8, 129.2, 128.5, 127.0, 67.3, 53.2, 37.6, 30.3, 29.1; optical rotation [α]_D²⁵ –5° (c 1, MeOH). Anal. Calcd for C₂₀H₂₁N₁O₅: C, 67.59; H, 5.96; N, 3.94. Found: C, 67.36; H, 5.98; N, 3.92.

Bis(Nα-amido-L-phenylalanine benzyl ester) Succinate (9). BOP (0.93 g, 2.1 mmol) was added to a stirred solution of **8** (0.71 g, 2 mmol) and L-Phe benzyl ester, *p*-toluenesulfonate salt (0.90 g, 2.1 mmol) in 20 mL of DMF, and the solution cooled to 0 °C. After stirring for 30 min, DIEA (0.54 g, 4.2 mmol) was added dropwise. The reaction mixture was warmed to room temperature and stirred overnight. The volatiles were removed under reduced pressure. The resulting oily residue was dissolved in EtOAc (100 mL) and washed with saturated aqueous NaHCO₃, 30% citric acid, and water. The organic layer was separated, dried with anhydrous Na₂SO₄, and filtered. Upon removal of half the solvent, the product precipitated out of solution as pure **9** (1.1 g, 93%): mp 160–161 °C; ¹H NMR (CDCl₃) δ 7.18 (m, 20H), 6.42 (d, 2H), 5.11 (q, 4H), 4.87 (m, 2H), 3.07 (m, 4H), 2.45 (m, 4H); ¹³C NMR (CDCl₃) 171.1, 170.9, 135.2, 128.8, 128.0, 126.5, 66.7, 52.9, 37.2, 30.8; optical rotation [α]_D²⁵ 23° (c 1, CHCl₃). Anal. Calcd for C₃₆H₃₆N₂O₆: C, 72.95; H, 6.12; N, 4.73. Found: C, 72.66; H, 6.08; N, 4.68.

(Nα-amido-L-phenylalanine) monosuccinate (10). Compound **10** was prepared by hydrogenation of its benzyl ester **8** (0.71 g, 2 mmol) over 10% Pd–C (100 mg) in MeOH using the same procedure as described for the preparation of **5a** except the reaction was stirred for 6 h prior to workup. Filtration of the catalyst and concentration of the filtrate gave a white solid. Column chromatography (LH-20 Sephadex, 10% EtOH/toluene) and recrystallization with 50% EtOAc/hexane gave pure **10** (0.5 g, 94%): mp 104–105 °C; ¹H NMR (CDCl₃ + 10% d₆-DMSO): δ 8.02 (br s, 2H), 7.20 (m, 5H), 6.67 (d, 1H), 4.77 (m, 1H), 3.13 (m, 2H), 2.52 (m, 4H); ¹³C NMR (CDCl₃ + 10% d₆-DMSO) 174.8, 173.3, 171.7, 136.6, 129.6, 128.4, 126.9, 53.3, 37.5, 30.9, 29.6; optical rotation [α]_D²⁵ 32° (c 1, MeOH). Anal. Calcd for C₁₃H₁₃N₁O₅: C, 60.22; H, 5.85; N, 5.01. Found: C, 60.12; H, 5.84; N, 5.03.

Bis(Nα-amido-L-phenylalanine) Succinate (11). Compound **11** was prepared by hydrogenation of its dibenzyl ester **9** (2.37 g, 4 mmol)

over 10% Pd–C (0.2 g) in MeOH using the same procedure as described for **5a** except the reaction was stirred for 1 h prior to workup. Filtration of the catalyst and concentration of the filtrate gave **11** as a white solid (1.64 g, 99%). An analytical sample was obtained by recrystallization from a (1/1/1) solution of MeOH/EtOAc/hexane: mp 195–196 °C; ¹H NMR (CD₃OD) δ 7.21 (m, 10H), 4.62 (m, 2H), 3.15 (m, 2H), 2.94 (m, 2H), 2.36 (m, 4H); ¹³C NMR (CD₃OD) 175.1, 174.7, 138.8, 130.7, 129.8, 128.1, 55.5, 38.8, 32.4; optical rotation [α]_D²⁵ 27° (c 1, MeOH). Anal. Calcd for C₂₂H₂₄N₂O₆: C, 64.07; H, 5.87; N, 6.79. Found: C, 64.08; H, 5.85; N, 6.76.

Bis(Nα-amido-L-phenylalanine *tert*-butyl ester) Maleate (12). L-Phenylalanine *tert*-butyl ester hydrochloride (2.21 g, 8.6 mmol) and maleic acid (0.46 g, 4 mmol) were combined in DMF (50 mL) and cooled to 0 °C. BOP (3.95 g, 8.9 mmol) was added, and the solution was stirred for 10 min. DIEA (2.07 g, 16 mmol) was added dropwise over 10 min. The reaction was warmed to room temperature and stirred overnight. The volatiles were removed under reduced pressure and the crude solid was dissolved in CH₂Cl₂ and washed successively with 1 N HCl, water, saturated NaHCO₃, and water. The organic layer was separated, dried over anhydrous MgSO₄, filtered, and concentrated to give a yellow oil (3.77 g). Flash column chromatography (30% ethyl acetate/hexane, R_f = 0.14) gave the pure di-*tert*-butyl ester **12** (1.13 g, 54%): mp 138–139 °C; ¹H NMR (CDCl₃) δ 8.40 (d, 2H, NH), 7.18 (s, 10H, aromatic), 6.01 (s, 2H, olefinic), 4.73 (m, 2H, CH), 3.10 (d, 4H, CH₂), 1.37 (s, 18H, *tert*-butyl); optical rotation [α]_D²⁵ 109° (c 1.5, CDCl₃). Anal. Calcd for C₃₀H₃₈N₂O₆: C, 68.94; H, 7.33; N, 5.36. Found: C, 68.88; H, 7.40; N, 5.30.

Bis(Nα-amido-L-phenylalanine *tert*-butyl ester) Fumarate (13). L-Phenylalanine *tert*-butyl ester hydrochloride (2.58 g, 10 mmol) and fumaric acid (0.58 g, 5 mmol) were combined in DMF (50 mL) and cooled to 0 °C. BOP (4.42 g, 10 mmol) was added, and the solution was stirred for 20 min. DIEA (2.86 g, 22 mmol) was added dropwise over 10 min. The reaction was warmed to room temperature and stirred overnight. The volatiles were removed under reduced pressure, and the crude solid was dissolved in 50 mL of EtOAc and washed successively with 30% citric acid, water, saturated NaHCO₃, and water. The organic layer was separated, dried over anhydrous MgSO₄, filtered, and concentrated to give an oil (3.77 g). Flash column chromatography (40% ethyl acetate/CHCl₃) gave the pure di-*tert*-butyl ester **13** (2.2 g, 84%): mp 161–162 °C; ¹H NMR (CDCl₃) δ 7.27 (m, 10H, aromatic), 6.96 (s, 2H, olefinic), 6.94 (d, 2H, NH), 4.91 (m, 2H, CH), 3.08 (d, 4H, CH₂), 1.47 (s, 18H, *tert*-butyl); ¹³C NMR (CDCl₃) 170.4, 163.5, 135.9, 133.0, 129.4, 128.3, 126.9, 82.5, 53.8, 37.8; optical rotation [α]_D²⁵ –29° (c 1, MeOH). Anal. Calcd for C₃₀H₃₈N₂O₆: C, 68.94; H, 7.33; N, 5.36. Found: C, 69.26; H, 7.54; N, 5.28.

Bis(Nα-amido-L-phenylalanine) Maleate (14). The bis *tert*-butyl ester **12** (1.03 g, 1.97 mmol) was cooled to 0 °C, and TFA (20 mL) was added dropwise under a nitrogen atmosphere. After 1 h the volatiles were removed under reduced pressure to give a white solid. Column chromatography (6% EtOH/toluene then increased to 14% EtOH/toluene on Sephadex LH-20) gave the pure bis acid **14** (0.80 g, 99%): ¹H NMR (CD₃OD) δ 7.22 (m, 10H, aromatic), 6.18 (s, 2H, olefinic), 4.70 (dd, 2H, CH), 3.21 (dd, 2H, diastereotopic CH₂), 3.00 (dd, 2H, diastereotopic CH₂); optical rotation [α]_D²⁵ 41° (c 1, MeOH). Anal. Calcd for C₂₂H₂₂N₂O₆: C, 64.38; H, 5.40; N, 6.83. Found: C, 64.53; H, 5.59; N, 6.65.

Bis(Nα-amido-L-phenylalanine) Fumarate (15). The bis *tert*-butyl ester **13** (1.04 g, 2.0 mmol) was cooled to 0 °C, and TFA (25 mL) was added dropwise under a nitrogen atmosphere. After 1 h the volatiles were removed under reduced pressure to give a white solid. Recrystallization from EtOAc/EtOH/hexane (1/1/1) gave the pure bis acid **15** (0.73 g, 90%): ¹H NMR (CD₃OD) δ 7.08 (m, 10H), 6.68 (s, 2H), 4.56 (m, 2H, CH), 3.06 (m, 2H), 2.81 (dd, 2H); ¹³C NMR (CD₃OD) 174.2, 166.3, 138.3, 133.7, 130.2, 129.4, 127.8, 55.4, 38.4; optical rotation [α]_D²⁵ 10° (c 1, MeOH). Anal. Calcd for C₂₂H₂₂N₂O₆: C, 64.38; H, 5.40; N, 6.83. Found: C, 64.06; H, 5.39; N, 6.76.

Acknowledgment. The authors wish to thank Emisphere Technologies for their generous funding of this research and the University of Florida Center for Structural Biology for access to their NMR services.